Laser-Induced Damage in Dielectrics with Nanosecond to Subpicosecond Pulses

B. C. Stuart, M. D. Feit, A. M. Rubenchik, B. W. Shore, and M. D. Perry
Lawrence Livermore National Laboratory, P.O. Box 808, L-443, Livermore, California 94550
(Received 24 August 1994)

We report extensive measurements of damage thresholds for fused silica and calcium fluoride at 1053 and 526 nm for pulse durations τ ranging from 270 fs to 1 ns. Qualitative differences in the morphology of damage and a departure from the diffusion-dominated $\tau^{1/2}$ scaling indicate that damage results from plasma formation and ablation for $\tau \leq 10$ ps and from conventional melting and boiling for $\tau > 100$ ps. A theoretical model based on electron production via multiphoton ionization, Joule heating, and collisional (avalanche) ionization is in good agreement with experimental results.

PACS numbers: 61.80.Ba, 42.70.–a, 71.38.+i

Laser-induced damage has been observed in transparent solids since the advent of powerful lasers and has been the subject of numerous studies over many years [1–5]. For pulses longer than a few tens of picoseconds, the generally accepted picture of bulk damage to defect-free dielectrics involves the heating of conduction band electrons by the incident radiation and transfer of this energy to the lattice. Damage occurs via conventional heat deposition resulting in the melting and boiling of the dielectric material. Because the controlling rate is that of thermal conduction through the lattice, this model predicts a $\tau^{1/2}$ dependence of the threshold fluence (energy/area) upon pulse duration τ [6], in reasonably good agreement with numerous experiments which have observed a τ^{α} scaling with $0.4 < \alpha < 0.5$ in a variety of dielectric materials from 100 ps to 10 ns [7].

Recently, the application of chirped-pulse amplification (CPA) [8] to solid-state lasers has enabled terawatt class systems producing subpicosecond pulses. Further increase in the peak power available from such systems [9] is now limited by damage to optical surfaces due to the intense short pulses. This duration is significantly shorter than the time scale for electron energy transfer to the lattice. As a result, damage caused by subpicosecond pulses is characterized by ablation, with essentially no collateral damage. Many applications, ranging from materials processing to biomedical technologies, could potentially benefit from the more localized energy deposition of short-pulse lasers.

In this Letter, we report extensive measurements of laser-induced damage thresholds for fused silica and calcium fluoride for pulses ranging from 270 fs to 1 ns. In each of these large-band-gap materials we observe a change in the damage mechanism and morphology for pulses shorter than 20 ps. Although we observe a deviation from $\tau^{1/2}$ scaling as reported by Du *et al.* [10], we find no evidence for an increase in damage threshold with decreasing pulse width. Instead, we observe a decreasing threshold associated with a gradual transition from the long-pulse, thermally dominated regime to an ablative regime dominated by collisional and multiphoton ionization, and plasma formation. A general theoretical model of laser interaction with dielectrics, based on multiphoton ionization, Joule heating, and collisional (avalanche) ionization, is shown to be in good agreement with the data in this short-pulse regime and over a broad range of laser wavelength. This model is consistent with the observations [11] of critical density plasmas produced by ultrashort pulses.

Experimentally, we utilized laser pulses generated by a 1053 nm Ti:sapphire CPA system [12]. Seed pulses of 100 fs from a Kerr-lens mode-locked oscillator were stretched to 1 ns and then amplified up to 60 mJ in a linear regenerative amplifier followed by a ring regenerative amplifier, both producing TEM_{00} Gaussian modes. The rms energy stability of the laser system was 3%. By changing the dispersive path length of our single-grating compressor, we obtained pulses of continuously adjustable duration from 0.4 to 900 ps. We performed damage measurements with laser spot sizes adjustable from 0.3 to 1.0 mm diameter. Light at 526 nm was generated by frequency doubling the compressed pulses in a thin (4 mm) KD^*P crystal.

The results presented here for fused silica were obtained with 1 cm thick "superpolished" samples exhibiting less than 1 nm rms surface roughness. We measured similar damage thresholds for a 200 μm thick fused-silica etalon, which was tested to examine any differences between thick and thin samples. The presence of surface cracks, nodules, or voids is known to increase the local field intensity by a factor of η^4, where η is the refractive index [2]. This increase takes place over a region comparable to the feature scale length a and is offset by convection of electrons away from the region. A simple estimate of convection shows that for picosecond pulses the local enhancement is insignificant for $a \leq 40$ nm. We thus believe our measurements are representative of a uniform fused silica surface. The surface quality of the relatively soft fluorides was much poorer than the fused silica samples.

We define damage to be any visible permanent modification to the surface observable with a Nomarski microscope. The smallest damage spots we could observe were

 0031-9007/95/74(12)/2248(4)$06.00

approximately 0.5 μm in diameter, an area 10^6 smaller than the laser spot size and nearly impossible to observe by other methods (e.g., degradation of transmission, scattered light, etc.). To avoid the complications of spatial and temporal distortion caused by self-focusing, group velocity dispersion, and self-phase modulation when propagating pulses through optical materials, we considered only front-surface damage. When it occurred, we were careful not to let rear-surface damage propagate to the front surface. Initial damage, at threshold, may have many forms: ablation of a few atomic layers; formation of a color center, shallow traps, or lattice defects; or melting of a very small volume. These weak effects are very difficult to detect. In order the "amplify" this damage to an easily observable size, and to minimize statistical uncertainty, we conducted our damage testing with multiple pulses of a given fluence on each site. This is in contrast to single-shot measurements reported by Du *et al.* [10], which required detection of a decrease in transmission or plasma emission caused by the single pulse. Many fluence levels (15–30) were examined above and below the damage threshold for a given pulsewidth in order to establish the threshold value.

Our measurements of the threshold damage fluence of fused silica and CaF_2 at 1053 nm as a function of laser pulse length (FWHM) are shown in Fig. 1. In the long-pulse regime ($\tau > 20$ ps), the data fit well by a $\tau^{1/2}$ dependence, characteristic of the transfer of electron kinetic energy to the lattice and diffusion during the laser pulse. The damage is thermal in nature and characterized by the melting and boiling of the surface [Fig. 2(a)]. The damage occurs over the entire area irradiated. For long pulses, heating of the lattice and subsequent thermal damage can occur without significant collisional ionization [13]. For pulses shorter than 20 ps, the damage fluence no longer follows the $\tau^{1/2}$ dependence and exhibits a morphology dramatically different from that observed with long pulses. The damage appears as a shallow fractured and pitted crater characteristic of a thin layer of material removed by ablation [Fig. 2(b)]. Furthermore, short-pulse damage is confined to a small region at the peak of the Gaussian irradiance distribution, where the intensity is sufficient to produce multiphoton ionization. With insufficient time for lattice coupling, there is no collateral damage. As a result, the damaged area can be many orders of magnitude smaller with short ($\tau < 10$ ps) pulses than with long pulses. For the case of fused silica shown in Fig. 2, the damage area produced by the 500 fs pulse was 2 orders of magnitude smaller than that produced by the 900 ps pulse.

Although the absolute damage fluence varies from material to material, all pure dielectrics (e.g., fluorides) and even multilayer mirrors we tested show a similar dependence on pulse width as observed for SiO_2. This behavior is to be expected, since all transparent dielectrics share the same general properties of slow thermal diffusion, rapid Joule heating, and fast electron-phonon scattering.

The theoretical description of damage with short pulses is simplified relative to that of long-pulse physics by two factors. First, the high intensities involved mean there is no need to invoke some arbitrary number of initial "seed" electrons [1–5,10,11,13]. Field-induced multiphoton ionization produces free electrons which are then heated rapidly by the pulse, resulting in further ionization due to collisions. Second, for these very short, intense pulses, conduction-band electrons gain energy from the laser field much faster than they transfer energy to the lattice. The actual damage occurs after the pulse has passed, when this electron energy is coupled into the lattice.

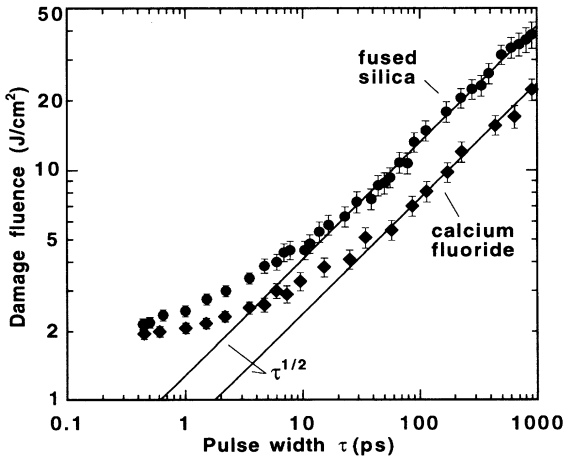

FIG. 1. Observed values of damage threshold at 1053 nm for fused silica (●) and CaF_2 (◆). Solid lines are $\tau^{1/2}$ fits to long pulse results. Estimated uncertainty in the absolute fluence is ±15%.

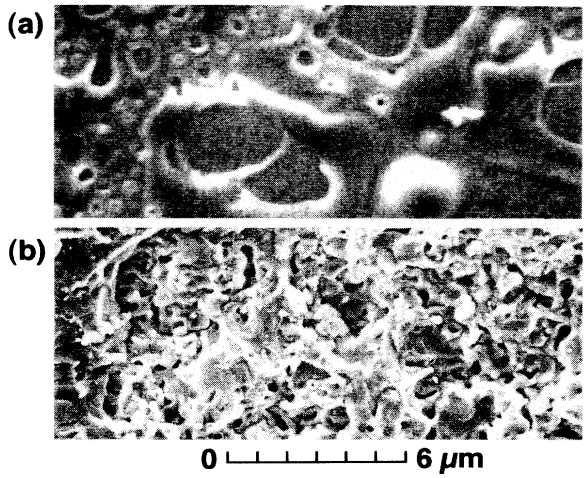

FIG. 2. Scanning electron micrograph of front-surface damage of fused silica produced by 1053 nm pulses of duration (a) 900 ps, showing melting, and (b) 500 fs, showing ablation and fracture.

Our model is based on a kinetic equation describing the time dependence of the electron energy distribution function. Since the impact ionization rate, like the other electron collision rates, is energy dependent, the actual absorption rate of laser energy requires integrating over the electron energy distribution. When the electrons are strongly driven, the energy distribution can differ substantially from a Maxwellian distribution.

For insulators or other materials with large band-gap energies ($U_I \gg \hbar\omega$), the heating and collisional ionization of conduction electrons can be described by a Fokker-Planck equation [5,14] for the electron distribution function $N(\varepsilon, t)$,

$$\frac{\partial N(\varepsilon,t)}{\partial t} + \frac{\partial}{\partial \varepsilon}\left[R_J(\varepsilon,t)N(\varepsilon,t) - \gamma(\varepsilon)E_p N(\varepsilon,t) - D(\varepsilon,t)\frac{\partial N(\varepsilon,t)}{\partial \varepsilon}\right] = S(\varepsilon,t), \quad (1)$$

where ε is the electron kinetic energy. The square bracket in Eq. (1) represents the change in the electron distribution due to Joule heating, the inelastic scattering of phonons, and electron energy diffusion. The heating rate of the electrons is taken as $R_J(\varepsilon,t) = \frac{1}{3}\sigma(\varepsilon)E_{\rm rms}(t)^2$, where $E_{\rm rms}(t)$ is the electric field and $\sigma(\varepsilon) = e^2\tau_m(\varepsilon)/m^*[1 + \omega^2\tau_m(\varepsilon)^2]$ is the ac conductivity of a conduction-band electron. Here, $1/\tau_m(\varepsilon)$ is the energy-dependent, electron-phonon transport (momentum) scattering rate. The rate of energy transfer from the electrons to the lattice is given by $E_p\gamma(\varepsilon)N(\varepsilon,t)$, where E_p is the energy of a typical phonon (0.03 eV) and $\gamma(\varepsilon)$ is the rate of electron-phonon energy transfer to the lattice. The scattering rates and effective mass ($m^* = m_e$) were taken from Arnold, Cartier, and DiMaria [16]. For fused silica $1/\tau_m = 10^{14}-10^{16}\,{\rm s}^{-1}$ and $\gamma = 10^{13}-10^{15}\,{\rm s}^{-1}$. The term $D(\varepsilon,t)\partial N/\partial\varepsilon$ represents electron energy diffusion with $D(\varepsilon,t) = 2\varepsilon R_J(\varepsilon,t)$.

The final term $S(\varepsilon,t)$ represents sources and sinks of electrons. Electrons reaching energies above the gap U_I cause impact ionization at a rate described by the Keldysh impact formula [15] $R_I(\varepsilon) = \chi(\varepsilon/U_I - 1)^2$, with the remaining energy equally divided between the newly born electrons. For fused silica, the proportionality constant is $\chi = 1.5\times 10^{15}\,{\rm s}^{-1}$ [16]. Including multiphoton ionization $R_p(t)$, we write the source as [14]

$$S(\varepsilon,t) = R_p(t) - R_I(\varepsilon)N(\varepsilon,t) + 4R_I(2\varepsilon + U_I)N(2\varepsilon + U_I, t). \quad (2)$$

At 1053 nm, we use the strong-field Keldysh ionization formula for eight-photon absorption [17], while at 526 nm, we use the measured four-photon absorption cross section $\sigma^{(4)} = 2\times 10^{-114}\,{\rm cm}^8/{\rm s}^3$ [1].

Numerical solutions of Eq. (1) for a constant laser intensity (>100 GW/cm^2) and no multiphoton ionization show that after a few tens of femtoseconds the electron distribution grows exponentially in magnitude without changing shape, $N(\varepsilon,t) = g(\varepsilon)\exp[\beta t]$. The distribution $g(\varepsilon)$ is non-Maxwellian. Note that for pulses at the damage threshold observed in Fig. 1, and durations less than 10 ps, the intensity is sufficiently high that the Joule heating rate R_J is much greater than the rate of energy transfer to the lattice γE_p. This results in an average collisional ionization rate β which is proportional to the laser intensity $\beta = \alpha I$. In this limit, free electron generation reduces to a simple rate equation $dN(t)/dt = \alpha I(t)N(t) + R_p(t)$. The constant $\alpha \approx 0.01\,{\rm cm}^2\,{\rm ps}^{-1}/{\rm GW}$ is found by numerically solving Eq. (1).

Figure 3 shows the evolution of electron density for a 11.7 TW/cm^2, 100 fs pulse. The pulse intensity and the electron density produced by multiphoton ionization alone are included for reference. Because multiphoton ionization is strongly intensity dependent, the electron production takes place principally at the peak of the pulse. For this 100 fs duration, multiphoton ionization produces a substantial amount of free electrons with only a small collisional avalanche required to achieve critical density. Critical density ($\approx 10^{21}$ cm^{-3}) is not produced until late in the pulse. Only this last part of the laser pulse will experience any strong absorption or reflection.

In Fig. 4, we compare our measured and calculated damage thresholds at both 526 and 1053 nm from 10 fs to over 10 ps. We chose the plasma critical density (i.e., strongly absorptive regime) as the theoretical indicator of

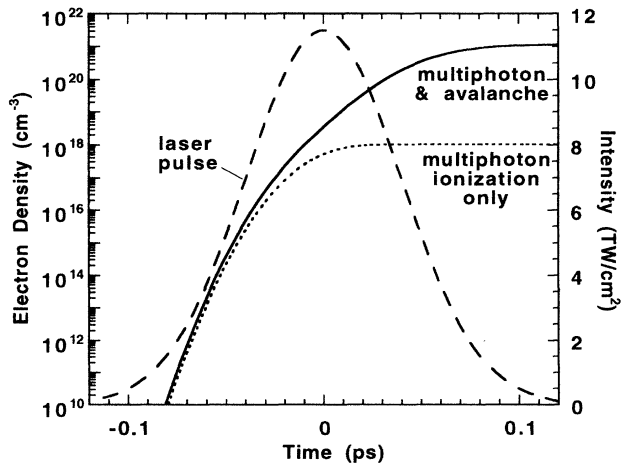

FIG. 3. Calculated evolution of free electron density for a 100 fs, 1053 nm pulse (dashed curve) of peak intensity 11.7 TW/cm^2 in fused silica. Multiphoton ionization (dotted curve) starts the avalanche; solid curve is total electron density including impact ionization.

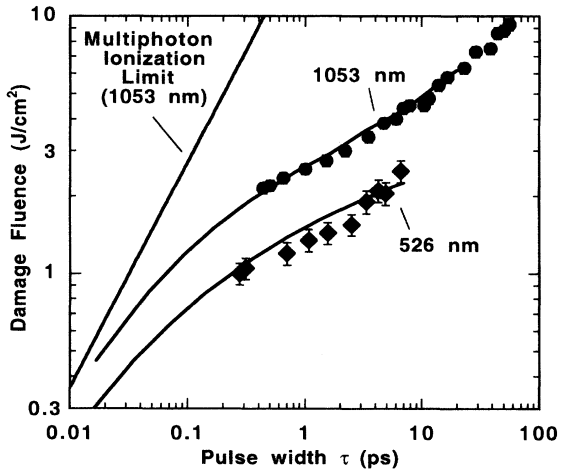

FIG. 4. Experimental and theoretical damage thresholds for fused silica at 1053 nm (●) and 526 nm (◆). The theoretical damage thresholds (solid curves) correspond to the formation of a critical density plasma ($\approx 10^{21}$ cm^{-3}), as discussed in the text. Relative errors in the experimental data are shown, estimated absolute error is ±15%.

macroscopic damage. The calculated threshold is not sensitive to this choice, decreasing by ≈20% for an electron density of 10^{19} cm^{-3} at which the energy density of conduction electrons equals the lattice binding energy. In addition to the good agreement between the model calculations and the measurements presented here, experiments by Daguzan *et al.* [18] and von der Linde and Schuler [19] with 620 nm, ≈100 fs pulses are also in good agreement with our calculations. For pulses less than 100 fs, the predicted damage threshold asymptotically approaches the multiphoton limit.

In conclusion, we observe a strong deviation from the long-pulse $\tau^{1/2}$ scaling of laser damage fluence for pulses below 20 ps in several transparent dielectric materials. The damage threshold continues to decrease with decreasing pulsewidth, but at a rate slower than $\tau^{1/2}$ in the range 0.1 to 20 ps. This departure is accompanied by a qualitative change in the damage morphology indicative of rapid plasma formation and surface ablation. The damage site is limited to only a small region where the laser intensity is sufficient to produce a plasma with essentially no collateral damage. A theoretical model, in which initial electrons provided by multiphoton ionization are further heated resulting in collisional (avalanche) ionization, predicts short-pulse damage thresholds in excellent agreement with our measurements. For extremely short pulses ($\tau < 30$ fs), multiphoton ionization alone provides the critical density of electrons.

We would like to thank F. Rainer and L. J. Atherton for providing the Nomarski microscope, and E. Lindsay for assistance with electron microscopy. J. H. Campbell, M. Kozlowski, D. Milam, and F. Rainer provided a wealth of data and advice on laser damage with long pulses. Finally, we would like to thank S. Herman for invaluable technical assistance. This work was performed under the auspices of the U.S. Department of Energy by Lawrence Livermore National Laboratory under Contract No. W-7405-ENG-48.

[1] S. C. Jones *et al.*, Opt. Eng. **28**, 1039 (1989).
[2] N. Bloembergen, IEEE J. Quantum Electron. **QE-10**, 375 (1974).
[3] E.g., *Laser Induced Damage in Optical Materials,* Proceedings of the Boulder Damage Symposium (U.S. Department of Commerce National Institute of Standards, Gaithersburg, 1969–93), Vol. 1–25.
[4] A. A. Manenkov and A. M. Prohkorov, Sov. Phys. Usp. **29**, 107 (1986).
[5] M. Sparks *et al.*, Phys. Rev. B **24**, 3519 (1981).
[6] R. M. Wood, *Laser Damage in Optical Materials* (Hilger, Boston, 1986).
[7] J. H. Campbell *et al.*, in *Laser Induced Damage in Optical Materials,* SPIE, **1441**, 444 (1990).
[8] D. Strickland and G. Mourou, Opt. Commun. **56**, 219 (1985); P. Maine *et al.*, IEEE J. Quantum Electron. **24**, 398 (1988).
[9] M. D. Perry and G. Mourou, Science **264**, 917 (1994).
[10] D. Du, X. Liu, G. Korn, J. Squier, and G. Mourou, Appl. Phys. Lett. **64**, 3071 (1994).
[11] B. V. Vu, O. L. Landen, and A. Szoke, Phys. Rev. E **47**, 2768 (1993).
[12] B. C. Stuart, S. Herman, and M. D. Perry, IEEE J. Quantum Electron **QE–31**, 528 (1995).
[13] X. A. Shen, S. C. Jones, and P. Braunlich, Phys. Rev. Lett. **62**, 2711 (1989).
[14] L. H. Holway, Jr. and D. W. Fradin, J. Appl. Phys. **46**, 279 (1974).
[15] B. K. Ridley, *Quantum Processes in Semiconductors* (Clarendon, Oxford, 1993).
[16] D. Arnold, E. Cartier, and D. J. DiMaria, Phys. Rev. A **45**, 1477 (1992).
[17] L. V. Keldysh, Sov. Phys. JETP **20**, 1307 (1965).
[18] Ph. Daguzan *et al.*, in Proceedings of Short Wavelength VI: Physics with High Intensity Pulses, St. Malo, France, 1994 (unpublished).
[19] D. von der Linde and H. Schuler, in Proceedings of Short Wavelength VI: Physics with High Intensity Pulses, St. Malo, France, 1994 (unpublished).

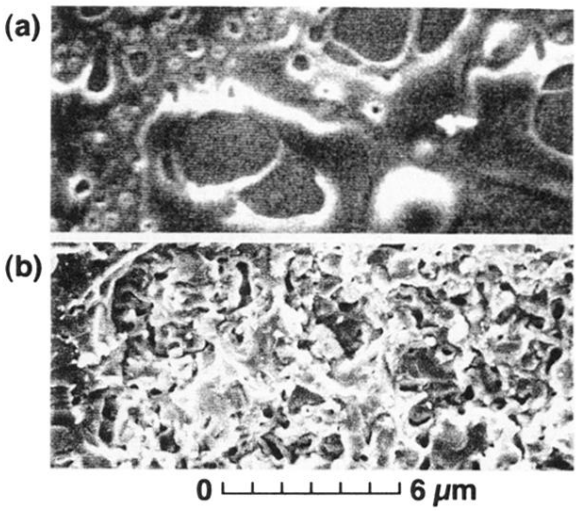

FIG. 2. Scanning electron micrograph of front-surface damage of fused silica produced by 1053 nm pulses of duration (a) 900 ps, showing melting, and (b) 500 fs, showing ablation and fracture.